Copper−Phthalocyanine Induced Reconstruction of Au(110)†

A. Cossaro,‡ D. Cvetko,§,|| G. Bavdek,|| L. Floreano,‡ R. Gotter,‡ A. Morgante,*,‡,⊥ F. Evangelista,# and A. Ruocco#

Laboratorio TASC dell'Istituto Nazionale per la Fisica della Materia, Basovizza SS-14, Km 163.5, I-34012 Trieste, Italy, Department of Physics, University of Ljubljana, Ljubljana, Slovenia, Jožef Stefan Institute, Ljubljana, Slovenia, Department of Physics, University of Trieste, Trieste, Italy, INFM unit of Roma Tre and Physics Department, University of Roma Tre, Via della Vasca Navale 84, 00146 Roma, Italy

Received: February 27, 2004; In Final Form: May 27, 2004

The structure of ultrathin Cu−phthalocyanine (Cu−Pc) film on Au(110) has been studied by means of several diffraction tecniques: helium atom scattering (HAS), low energy electron diffraction (LEED) and grazing incidence X-ray diffraction (GIXD). HAS has been used to measure the long range order of the organic overlayer, whereas LEED at 200 eV has been used to probe the corresponding substrate reconstruction. At the monolayer coverage, the Au(110) substrate displays a reconstruction with a 3-fold periodicity along the [001] direction, whose structure has been studied by out of plane GIXD and variable polarization X-ray absorption near edge spectroscopy (XANES). We found the structure of the substrate unit cell to be an asymmetric shallow (1 × 3) reconstruction with the Cu−Pc molecules tilted by an angle of ∼32° from the (110) surface plane.

I. Introduction

Metal-phthalocyanines (M−Pc) are planar molecules formed by conjugated aromatic macrocycles (four pyrrolic and four benzene rings) where the central metal atom is surrounded by four N atoms. Their high thermal and chemical stabilities make them well suited materials for the preparation of electronic devices, like organic LEDs, solar cells, thin film transistors, and gas sensors.[1−3] The possibility of choosing the host metal atom gives a further degree of freedom in tailoring the optical and electronic properties of the material. M−Pcs have been observed to grow and form two dimensional films on a number of ordered as well as amorphous substrates.[3] Tailoring the growth crystalline structure and/or choosing the growth plane orientation by appropriately selecting the substrate gives a further possibility of preparing electronic devices with the required electronic and optical properties. Moreover, the degree of crystalline order and molecular orientation reached during deposition also determines the transport properties of thin organic films. To this end, it is essential to obtain an accurate control of the relevant growth conditions.

In the low coverage range, the orientation of the M−Pc molecules can be driven by a proper choice of a reactive substrate. When metal surfaces are considered, the delocalization of π orbitals in the aromatic rings of M−Pc is expected to favor a flat lying adsorption geometry. One expects the driving force for molecule adsorption on metals to be the maximization of the contact area with the substrate. In fact, a flat growth of the first organic layers has been observed for a few M−Pcs on several metals [Cu−Pc/Au(100),[4] Cu−Pc/Au(111),[5] Cu−Pc/Al(100),[6] Sn−Pc/Ag(111),[7] Ni−Pc/Cu(100)[8]]. Along with this argument, the orientation of the molecules can be affected by the surface roughness,[9] and adsorption at the step edges on Au(111) has been demonstrated to effectively change the azimuthal orientation of Cu−Pc molecules on narrow terraces.[10] This indicates the possibility of exploiting highly corrugated crystal surfaces to drive the orientation of a growing overlayer on an otherwise poorly interacting substrate.

Following this guideline, we have studied ultrathin Cu−Pc overlayers deposited in a vacuum on Au(110). We have chosen the Au(110) surface for its strongly anisotropic structure. The clean Au(110) surface displays a (1 × 2) reconstruction, where every second atomic row (extending along [1$\bar{1}$0]) is missing (missing row model,[11] MR), forming deep troughs across the [001] direction. These troughs locally expose (111) microfacets tilted by 35° from the (110) plane, which may also favor an overlayer formation with tilted molecular alignement. In addition, higher order (1 × *n*) reconstructions of the Au surface are energetically very close to the (1 × 2) ground structure[12] and can be effectively induced by crystal impurities[13,14] or gas adsorption.[15] This substrate represents a very promising template to grow unidimensional organic structures, where molecules are expected to line up along the surface troughs (whose width of 8 Å is larger than the covalent diameter of aromatic rings). As a matter of fact, ordered molecular phases of sexithiophene[16,17] (T6) and perylene[18] on Au(110) have been obtained with a series of commensurate phases displaying coverage dependent periodicities along the [001] direction. Pentacene has been also reported to yield a 3-fold substrate reconstruction along the [001] direction at the saturation of the first layer on Au(110).[19]

Recently, ultrahigh vacuum (UHV) deposition of Cu−Pc molecules on the (1 × 2)-Au(110) surface has been found to form ordered commensurate phases in the monolayer thickness range. In fact, a LEED study by Evangelista et al.[20] reported

† Part of the special issue "Gerhard Ertl Festschrift".

‡ Laboratorio TASC dell'Istituto Nazionale per la Fisica della Materia.
§ University of Ljubljana.
|| Jožef Stefan Institute.
⊥ University of Trieste.
University of Roma Tre.
* Corresponding author: Fax: +39-040-226767. E-mail: morgante@tasc.infm.it.

10.1021/jp049108h CCC: $27.50
Published on Web 07/21/2004

that Cu−Pc molecules line-up along the [1$\bar{1}$0] direction (i.e., parallel to the Au missing row troughs) yielding a 5-fold periodicity. It has been further observed that this overlayer induces a surface symmetry with 3-fold periodicity along the [001] direction, thus forming an overall (5 × 3) phase. While the 5-fold periodicity along the [1$\bar{1}$0] (corresponding to 14.4 Å) can be easily understood in terms of molecular ordering in long chains (the Cu−Pc length is 13.8 Å), the 3-fold periodicity along the [001] (corresponding to 12.2 Å) suggests a tilted adsorption geometry. The most energetically favored (1 × 3) reconstruction of Au(110) is an extended missing row (called also deep MR), where profound troughs are formed (down to the fourth inner layer), which locally expose (111) microfacets.[21] This kind of substrate reconstruction was proposed for the 3-fold phase of perylene[18] and T6[17] on Au(110). This model has been also brought forward to the 4-fold phase of perylene/Au(110), where perylene was proposed to be adsorbed within the troughs of a five-layer-deep missing row reconstruction of Au(110).[18] Yet, these interpretations were based on STM topographic images of the ordered phases, and a thorough structural study of the substrate is still missing.

In this paper we present a detailed structural study of the Cu−Pc/Au(110) monolayer phase, corresponding to the previously reported (5 × 3) symmetry, and determine the nature of the 3-fold substrate phase. We have employed various experimental techniques able to determine the substrate structure, molecular orientation and long rang order. We exploited the complementary probing depths of HAS, LEED and GIXD experimental techniques to disentangle the information from the organic overlayer and that from the Au(110) substrate. In particular, GIXD measurements were used to determine the type and structure of the induced Au(110) reconstruction, whereas polarization dependent XANES measurements were used to determine the spatial orientation of the Cu−Pc molecular plane. Quite surprisingly, the molecules are indeed found to be tilted by ∼32° from the surface, but the substrate reconstruction is found to be a shallow (1 × 3) missing row structure. This finding is indicative of an energy expensive rearrangement of the substrate with a large mass transport at the surface, indicating that the interaction of the Cu−Pc molecules with the substrate is quite strong.

The quantitative estimation of the strength of the molecule-substrate interaction is lacking, yet the formation of the interface states in the valence band spectra, reported for the early stages of the Cu−Pc/Au deposition,[20] also evidences that the Cu−Pc molecules are not simply physisorbed on the Au substrate (i.e., of the van der Waals type) but instead interact strongly with the substrate, where the molecular electronic states hybridize with the Au surface states.

II. Experimental Section

Two different experimental apparati have been used for the present study. Helium and electron diffraction measurements have been taken with the HAS apparatus at the INFM-TASC Laboratory, which is described in detail elsewhere.[22] The HAS apparatus has been now equipped with a new hemispherical electron spectrometer (150 mm mean radius) and it has been modified to be attached at the ALOISA branchline (130−1300 eV photon energy range) for real time HAS and X-ray photoemission (XPS).[23] At present, the new spectrometer has been used in conjunction with an electron gun (for electron diffraction) and a He discharge lamp (for valence band spectroscopy, UPS).

Either He or electron diffraction patterns can be taken in real time during Cu−Pc evaporation. In both cases, one-dimensional diffraction patterns are acquired by polar rotation of the sample, which is mounted on a six-degrees of freedom VG CTPO manipulator (0.01° accuracy on each rotation axis). The sample temperature can be varied by liquid nitrogen cooling and radiative heating of the sample holder. The Cu−Pc molecules are evaporated from a boron nitride Knudsen cell hosted inside a cryo-panel. Cu−Pc has been evaporated with deposition rates on the order of one monolayer (ML) per hour. A few UPS and HAS spectra have been taken simultaneously during the CuPc evaporation at 300 K substrate temperature. All UPS spectra reproduce nicely the valence band spectrum evolution reported on the same system by Evangelista et al.[20] These results confirm the purity, cleanliness and composition of the evaporated material.

X-ray diffraction, photoemission, and absorption spectroscopy measurements have been performed at the ALOISA beamline[23] of the INFM-TASC Laboratory installed at the Elettra Synchrotron (Trieste, Italy). The ALOISA beamline, thanks to its unique monochromator, can provide photons in a very large energy range spanning from 130 to 8000 eV,[24] thus allowing to perform both photoelectron spectroscopies and GIXD. Also the experimental chamber exploits a unique design which allows to freely rotate in UHV (base pressure in the 10^{-11} mbar range), both energy electron analyzers and X-ray detectors independently from the sample. The latter is mounted on a modified CTPO VG manipulator, which allows to transfer the sample between the HAS apparatus and the ALOISA chamber with the same sample holder. The same Knudsen cells of the HAS apparatus have been also used in the ALOISA chamber, where a RHEED system was used to monitor the sample during Cu−Pc evaporation, for comparison with the LEED patterns taken in the HAS apparatus. A quartz microbalance was used to adjust the evaporation rate. The GIXD patterns have been collected by an energy resolved Si diode (by Eurisys). All GIXD diffraction measurements have been taken at a photon energy of 7000 eV and with the incidence angle fixed to 0.5°. From the in plane fractional peak profiles we obtained information about the domain size of the reconstructed surface.

Photoemission spectra have been measured in transverse magnetic polarization at normal emission with a 33 mm hemispherical spectrometer.[25] A photon energy of 500 eV has been used to measure the C 1s photoemission peak, with an overall energy resolution of ∼200 meV. A channeltron was used to measure the total yield absorption spectroscopy across the Cu $L_{2,3}$ thresholds (Cu 2p) at 952 and 933 eV binding energy. The photon energy scans of the ALOISA monochromator were performed with a photon energy resolution of 300 meV. A series of XANES spectra were collected as a function of the polar angle between the X-ray scattering plane and the photon polarization $\vec{\epsilon}$. This is achieved in the specific experimental setup of the ALOISA beamline by rotating the sample around an axis coincident with the X-ray beam, while keeping the X-ray incidence angle fixed.

III. Results and Discussion

A. XPS and XANES. An XPS spectrum of the C 1s core level collected for a 3 Å Cu−Pc film (as estimated from the quartz microbalance) is reported in Figure 1. For this coverage the RHEED and GIXD scans yield a 3-fold periodicity along the [001] direction, in agreement with the LEED observation of a (5 × 3) phase by Evangelista et al.,[20] and we can assume that the Cu−Pc molecules are all in contact with the Au substrate. In this case we expect that any effect due to the molecule-substrate interaction should show up in the XPS

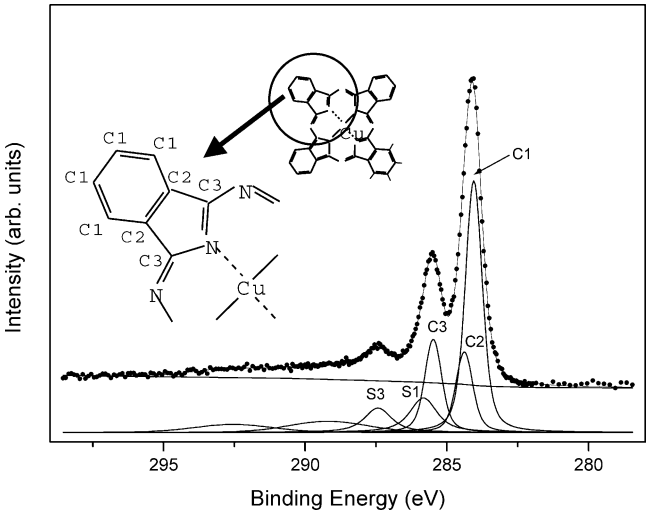

Figure 1. X-ray photoemission spectrum of the C 1s core level at the monolayer Cu−Pc coverage taken with the photon energy of 500 eV. Experimental points (markers) have been fit to multicomponent spectrum (full line = total fit). Different components belong to different C atoms within the molecule are shown and denoted. Inset: the real space model of the Cu−Pc molecule with the central Cu atom surrounded by four nitrogens. Left hand side of the inset is a magnified quadrant of the Cu−Pc molecule. The carbon atoms belonging to benzene (C1) and pyrrolic (C2 and C3) ring are denoted.

spectra. The XPS spectrum presented in Figure 1 displays two main peaks, arising from the two inequivalent carbon atoms belonging to the pyrrolic (labeled C3 in Figure 1) and benzene rings (C1), and a shake-up satellite (S_{C3}) stemming from the HOMO−LUMO transition in the molecule.[26−28] A more detailed analysis reveals the presence of other two components, labeled S_{C1} and C2. The component S_{C1} on the high binding energy side of the pyrrolic carbon C3 is acknowledged to be the shake-up satellite of the benzene C1 atoms,[29−31] whereas the highest binding energy shake-up satellite S_{C3} is originated by the pyrrolic C3 atoms. The fifth component C2 might be originated from inequivalent carbon atoms in the benzene rings, but recent density functional calculations for the similar Pb−Pc molecule have shown that the energy shift between inequivalent benzen atoms is much smaller than the observed C1−C3 splitting. The C2 component has been rather attributed to the vibrational coupling with the C−H stretching mode.[31]

In our case, the observed spectrum is indeed quite similar to the photoemission structures observed for the bulklike Cu−Pc, so it seems that the substrate does not affect the molecular electronic structure in a dramatic way, thus suggesting only a weak interaction of molecules with the susbtrate, at least when compared with other substrates such as Al[32] or Si.[28] To gain information on the molecular orientation, we have measured the Cu $L_{2,3}$ X-ray absorption edge. The absorption spectrum is composed of a main line (commonly called white line) and some satellites, as already observed experimentally on other substrates[8,28] and recently calculated by a density functional approach.[34] These calculations demonstrate that the white line is due to an atomic-like transition from the Cu 2p to an empty state, which is mainly of Cu $3d_{x^2-y^2}$ character and whose dipole momentum lies in the molecular plane. This transition is thus strongly enhanced when the radiation electric field vector lies in the molecular plane. We have therefore been able to use the polar angular dependence of the L_3 white line to determine the molecular orientation at the surface. The intensity of the L_3 white line as a function of the polar angle for a Cu−Pc coverage corresponding to the monolayer phase are reported in Figure 2.

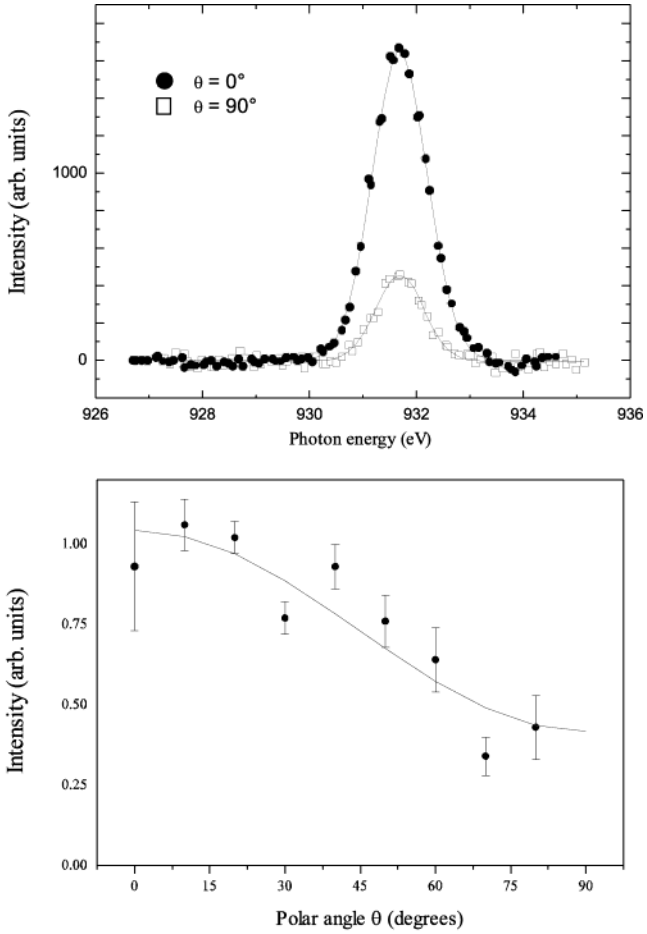

Figure 2. Upper panel: normalized Cu L_3 X-ray absorption spectrum (NEXAFS) as a function of the photon energy taken for two different polar angles (θ) (see text for details). Lower panel: The integrated NEXAFS intensity (markers) as a function of θ for the monolayer 5 × 3 Cu−Pc/Au(110) surface. The best fit (full line) with the model intensity given by eq 2 yields the molecular tilt angle from the surface as $\gamma = 32° \pm 3°$.

Every point reported in Figure 2 represents the integrated peak intensity after the normalization procedure. This includes the division by the photon flux (I_0) and the division by a reference signal below the L_3 edge, which takes into account, as a function of the polar angle θ, both the variable field of view of the analyzer and the variable sample area illuminated by the light. In the model used to interpret the data we also consider the incidence angle α of the light (that was kept fixed to 7°) and the orientation of the molecules with respect to the [001] surface direction (the azimuthal angle ψ). The overal normalized intensity, accounting for these contributions, can be written as[33]

$$1 - |\vec{N}\cdot\vec{\epsilon}|^2 = S(1 - |\sin\gamma\sin\psi\sin\alpha + \sin\gamma\cos\psi\cos\theta + \cos\gamma\sin\theta\cos\alpha|^2) \quad (1)$$

where $\vec{N}$ is a unit vector normal to the molecular plane and S is a scale factor, while γ represents the angle between the molecular plane and the substrate surface. Here the 2-fold symmetry of the substrate must be taken into account; in particular, for our choice of the reference frame, XANES data have been collected for $\psi = \pm 90°$, so that the expression 1 becomes

$$1 - |\vec{N}\cdot\vec{\epsilon}|^2 = S\,(1 - |\sin\gamma\sin\alpha + \cos\gamma\sin\theta\cos\alpha|^2) \quad (2)$$

where only the S scale factor and the γ angle are free fitting

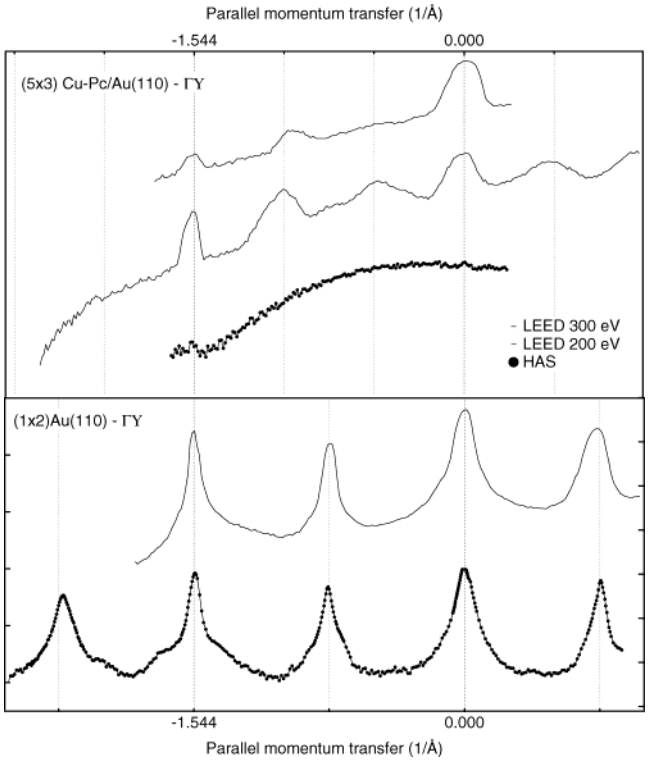

Figure 3. Diffraction patterns along Γ*Y*. HAS (markers) and LEED (full line) for the clean 1 × 2 reconstructed Au(110)(lower panel) and for the 5 × 3 Cu−Pc/Au(110) phase deposited at 300 K substrate temperature. The upper and the lower LEED curve is taken with 200 and 300 eV kinetic energy, respectively. All curves are given on a logarithmic scale and have been displaced vertically, for clarity.

parameters. The best fit to the experimental points, yielding $\gamma = 32° \pm 3°$, is reported as a full line in Figure 2.

B. LEED, HAS, and GIXD. The structure and order of the Cu−Pc monolayer phase has been addressed by simultaneous LEED and HAS diffraction experiments. HAS intensity has been collected with a beam energy $E_{He} \sim 19$ meV (wavelength $\lambda = 1.02$ Å) and energy resolution of $\Delta E/E \sim 0.02$, and LEED pattern has been measured with a kinetic energy betwen 200−300 eV. The overall HAS angular resolution is ∼0.135° corresponding to a transfer width at the surface exceeding 450 Å.

A series of HAS and LEED scans along Γ*Y* (i.e., with the scattering plane aligned in the [001] direction), direction have been taken during the Cu−Pc deposition with the substrate strictly held at a surface temperature of 300 K. Both HAS and LEED patterns display various periodicities during the overlayer growth, with LEED eventually reaching a 3-fold pattern in the [001] direction, which upon further deposition only decreases in intensity. We have therefore attributed this stage to a monolayer saturation coverage in agreement with previous studies of the same system, where a (5 × 3) LEED pattern was observed with 45 eV electron kinetic energy.[20]

Figure 3 shows both HAS and LEED scans taken for the monolayer phase obtained by Cu−Pc deposition at room temperature. For comparison, the patterns along the Γ*Y* surface direction are given also for a clean and well ordered (1 × 2)-Au(110) surface (lower panel). The (1 × 2)-Au(110) diffraction pattern displays a characteristic half-integer peak at 0.77 Å^{-1} due to the 2-fold missing row reconstruction. Well ordered terraces extend over 250 Å, as judged from the widths of the integer and half-integer diffraction peaks. Figure 3 upper panel displays LEED and HAS patterns of the monolayer phase. We

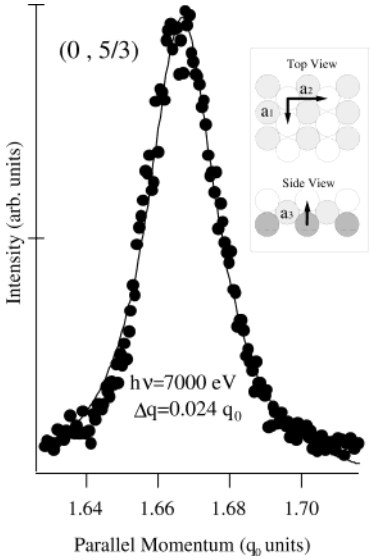

Figure 4. In plane X-ray surface diffraction peak characteristic of the 5 × 3 Cu−Pc monolayer phase taken with the photon energy of 7000 eV (markers). The full line is a best fit Lorentzian curve yielding a peak width $\delta q = 0.024 q_0$, where q_0 is the rlu vector ($2\pi/a_2$). The resulting 3-fold order correlation length exceeds 170 Å. Inset: Au-(110) unreconstructed unit cell; a_1 and a_2 are surface unit vectors of the unreconstructed surface along the [1$\bar{1}$0] and [001] direction, respectively, and a_3 is twice the (110) interplanar distance. The vector lengths are $a_1 = a_3 = 2.88$ Å and $a_2 = 4.08$ Å.

observe that, whereas LEED displays a 3-fold structure, the HAS diffraction pattern shows almost no diffraction, not even when taken at low temperatures (120 K), where the intensity attenuation due to the Debye−Waller thermal vibrations is strongly reduced (see Figure 3). The organic overlayer formed at 300 K deposition is observed to lack a significant long range order, although a substantial degree of Cu−Pc ordering could be observed in HAS patterns, when the Cu−Pc overlayer is grown at some tens degrees higher substrate temperature (not shown here). LEED patterns at 200 eV electron kinetic energy are less sensitive to the disorder of the organic overlayer and the observed 3-fold periodicity along Γ*Y* can be attributed to a periodic rearrangement of the substrate.

The overall (5 × 3) symmetry of the Cu−Pc monolayer phase, as reported by Evangelista et al.,[20] is hence attributed to two contributions: a 3-fold substrate reconstruction along the [001] direction and a 5-fold periodicity along the [1$\bar{1}$0] direction arising from the arrangement of Cu−Pc molecules, which line up parallel to the (×3) substrate troughs.

The structure of the Au(110) substrate has been determined by a GIXD study of the Cu−Pc monolayer phase (nominal thickness of 3 Å), where XPS and XANES spectra were also taken. In Figure 4, the (0, $^5/_3$) in plane reflection is reported as a function of the parallel momentum transfer expressed in units of $q_2 = 2\pi/a_2$. The notation used for indicating the X-ray reflections are referred to the unit cell depicted in the inset of Figure 4. The inverse of the peak width yields a 170 Å spatial extension of the average domain with 3-fold symmetry along [001], whereas the same analysis performed on the (0, $^3/_2$) reflection on a clean missing row Au surface yields an (1 × 2) domain size of 740 Å.

The real space structure of the 1 × 3 unit cell of the reconstructed Au substrate has been analyzed by measuring the out of plane X-ray diffraction peaks. Six nonequivalent rod scans (in total 292 reflections) along the [010] direction have been taken, on both bulk and reconstruction peaks. Figure 5 shows the integrated diffraction peak intensities as a function of the

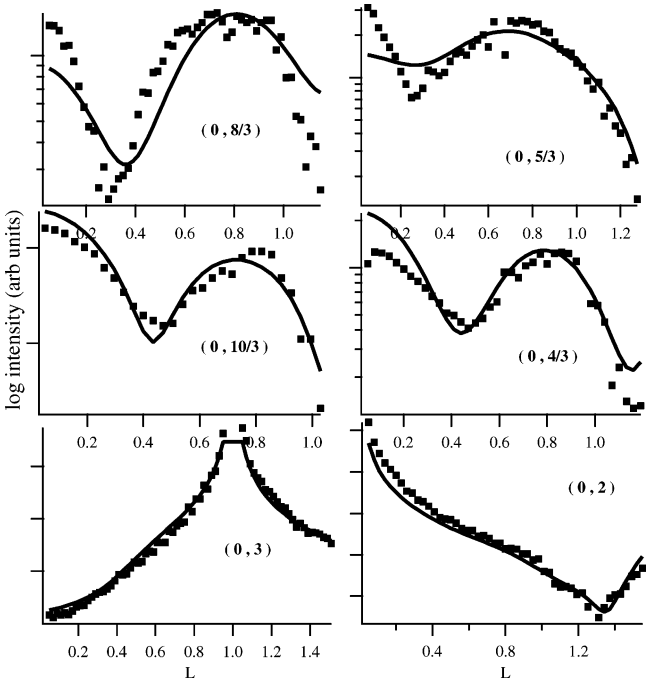

Figure 5. Six nonequivalent rod scan analysis of the out of plane GIXD for the 5 × 3 Cu−Pc structure. *L* denotes the perpendicular momentum transfer in units of $2\pi/a_3$. Each experimental point (markers) is obtained as an angle integrated intensity of a single diffraction peak at a given *L*. Full line is the best overall fit to the experimental data obtained with the "ROD" simulation program,[35] by assuming the "shallow" Au(110) 1 × 3 reconstructed unit cell. The structural best fit parameters are given in Table 1.

vertical momentum transfer (rod scans) and the corresponding best fit calculated curves obtained with the numerical "ROD" program.[35] No overlayer molecules have been included in the numerical calculations and only the position of the Au substrate atoms has been varied in the fitting procedure. This assumption is based on two evidences: (a) as indicated by LEED and HAS, the 3-fold periodicity mainly arises from a substrate distortion, whose atoms have an atomic scattering factor much larger than that of the low *Z* atoms, which mainly constitute the Cu−Pc molecules; (b) the absence of 3-fold periodicity in the HAS patterns along Γ*Y*, which is only sensitive to the outermost surface charge density, implies a strongly disordered overlayer;[39] i.e., no coherent contribution to the X-ray diffraction due to Cu−Pc molecules is expected in the 3-fold pattern.

The best fit results are summarized in Figure 6 and Table 1. Filled markers in Figure 6 indicate the "shallow" Au (1 × 3) reconstructed unit cell, where two [1$\bar{1}$0] Au rows out of three along the [001] are missing. We have also considered the other possible missing row 3-fold substrate reconstruction, where the central atomic row (number 3 in Figure 6) is missing, exposing two (111) microfacets within the unit cell. The (0, 3) rod scan data and the simulations for the two types of unrelaxed (1 × 3) unit cells are reported in Figure 7. It is evident that the shallow cell reproduces the experimental data much better. Moreover the best fit parameters obtained for the "deep" (1 × 3) unit cell yield a poor quality fit, which also results in unphysical cell distortions.

The displacements of the single atoms of the shallow (1 × 3) unit cell obtained from the best fit to all six nonequivalent X-ray rod scans are reported in Table 1. An asymmetrical relaxation of the susbtrate unit cell is required for the best fit. As a consequence, the fitting curve has been obtained by an incoherent sum of two 180° azimuthally rotated unit cells.

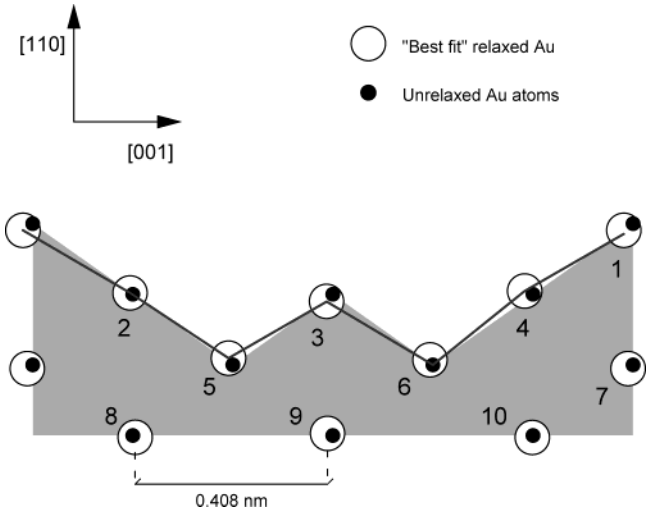

Figure 6. Schematic representation of the unrelaxed (filled markers) and best fit (open circles) atomic positions of the "shallow" Au(110) 1 × 3 reconstructed unit cell (in scale). The same atom indexing is used in Table 1. See text for details.

TABLE 1: Atomic Displacements from the Ideal Bulk Position of the Au Atoms in the Shallow (1 × 3) Unit Cell

atom index	in plane displacement	out of plane displacement
1	−0.19	−0.13
2	−0.06	0.03
3	−0.13	−0.14
4	−0.17	0.07
5	−0.09	0.13
6	−0.06	0.10
7	−0.10	−0.08
8	0.05	−0.04
9	−0.11	0.04
10	−0.01	−0.04

[a] Displacements are given in Å with an accuracy of ±0.03 Å. The atom indexes correspond to labeling of Figure 6.

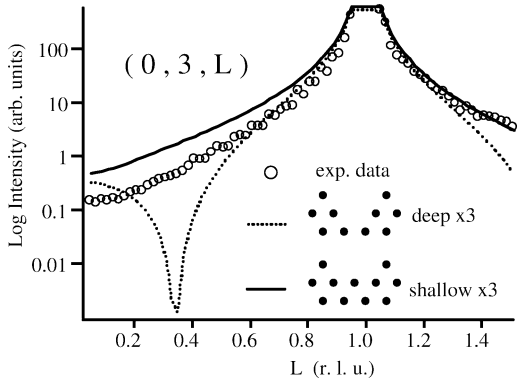

Figure 7. (0, 3) integer order rod scan of the 5 × 3 Cu-Pc monolayer phase. The simulated intensity for both, the unrelaxed "shallow" (full line) and unrelaxed "deep" (dotted line) (1 × 3) reconctructions is shown for comparison. A sketch of the structure of the two models along the [001] direction is also shown.

The shallow (1 × 3) unit cell may be viewed as a pair of up−down correlated monatomic steps, containing a local (1 × 1) unit, whereas the deep (1 × 3) unit cell is a pair of up−down correlated steps made of (111) microfacets.[36] The fact that the shallow (1 × 3) Au reconstruction is preferred in the presence of Cu−Pc molecules is quite interesting since, on a clean Au(110) surface, the deep (1 × 3) reconstruction is expected to be more favorable.[21] This hierarchy of the energy of Au(110) surface defects is experimentally confirmed, since

the (1 × 3) step type has been observed to dominate over the (1 × 1) type at the Au(110) roughening transition, which takes place by proliferation of monatomic steps.[37] Cu−Pc deposition on Au(111) has also been reported to favor molecular alignement along the preexisting monatomic steps.[10] On the bare Au(110) surface, monatomic steps mainly extend along the [1$\bar{1}$0],[37,38] so it may not be surprising that Cu−Pc molecules, not only align along the [1$\bar{1}$0], but also induce a particular substrate reconstruction in which the (1 × 3) unit cell is formed by an up−down correlated pair of monatomic steps along [1$\bar{1}$0].

The XANES measurements at the Cu L_{23} edge as a function of polar and azimuthal orientation demonstrate that the Cu−Pc molecules lie along the (1 × 3) Au(110) troughs, tilted by 32° from the surface. This finding is further consistent with the observed asymmetric relaxation of the Au(110) shallow (1 × 3) unit cell. In fact, in both XANES and GIXD analysis an incoherent sum of the two equivalent molecular tilt angles, and substrate unit cell relaxations, produced the best fit to the experimental data.

IV. Conclusions

In conclusion, we have studied the structure and order of the Cu−Pc organic overlayer deposited at 300 K on the Au(110) substrate. It is observed that the (1 × 2) missing row reconstruction of the bare substrate is lifted by the organic overlayer into a shallow (1 × 3) reconstruction. Unlike the Au(110) substrate, the organic overlayer formed at 300 K deposition has been observed to lack a significant long range order, although a substantial degree of Cu−Pc ordering could be observed when the Cu−Pc overlayer is grown at higher substrate temperatures. It is due to the Cu−Pc molecular lining-up in correlated chains along the [1$\bar{1}$0] that the overall symmetry of the Cu−Pc monolayer phase eventually yields a (5 × 3) symmetry.

The type of substrate reconstruction at the monolayer phase has been determined by GIXD as a "shallow" 3-fold reconstruction involving only the three outermost Au(110) layers. The geometrical relaxations of the Au atoms within the (1 × 3) unit cell have been also determined. Significant inward and sideward atomic displacements have been found with a broken reflection symmetry across the missing row, consistent with the fact that Cu−Pc molecules lie tilted within the Au troughs. Indeed, polarization dependent XANES measurements of the Cu−Pc molecular orientation evidence that molecules lie with the molecular plane along the [1$\bar{1}$0] and tilted by 32 ± 3° from the surface (110) plane.

Although little evidence of molecule-substrate interaction could be observed in the XPS measurements of the carbon 1s core level spectrum, the type of induced (1 × 3) Au(110) substrate unit cell suggests a rather strong Cu−Pc overlayer coupling to the substrate reconstruction. This finding is in agreement with the formation of interface states in the system valence band, which was reported to take place at the early deposition stage of Cu−Pc.[20] Current experiments have shown that these interface states at the (5 × 3) monolayer phase also display a dispersion along ΓX with a 5-fold periodicity.[40]

Acknowledgment. This research has been partially funded by MURST cofin2003 028141.

References and Notes

(1) Silinsh, E. A.; Čapek, V. *Organic molecular crystals*; AIP Press: New York, 1994.

(2) Joachim, C.; Gimzewski, J. K.; Aviram, A. *Nature (London)* **2000**, *408*, 541.

(3) Schreiber, F. *Phys. Stat. Solidi A* **2004**, *201*, 1037.

(4) Park, K. T.; Miller, A.; Klier, K.; Opila, R. L.; Rowe, J. E. *Surf. Sci.* **2003**, *529*, L285.

(5) Fritz, T.; Hara, M.; Knoll, W.; Sasabe, H. *Mol. Cryst. Liq. Cryst.* **1994**, *253*, 269.

(6) Ruocco, A.; Donzello, M. P.; Evangelista, F.; Stefani, G. *Phys. Rev. B* **2003**, *67*, 155408.

(7) Lackinger, M.; Hietschild, M. *Surf. Sci.* **2002**, *520*, L619.

(8) Dufour, G.; Poncey, C.; Rochet, F.; Roulet, H.; Iacobucci, S.; Sacchi, M.; Yubero, F.; Motta, N.; Piancastelli, M. N.; Sgarlata, A.; De Crescenzi, M. *J. Electron Spectrosc. Relat. Phenom.* **1995**, *76*, 219.

(9) Nakamura, M.; Morita, Y.; Mori, Y.; Ishitani, A.; Tokumoto, H. *J. Vac. Sci. Technol. B* **1996**, *14*, 1109.

(10) Chizhov, I.; Scoles, G.; Kahn, A. *Langmuir* **2000**, *16*, 4358.

(11) Moritz, W.; Wolf, D. *Surf. Sci.* **1986**, *163*, L655.

(12) Ercolessi, F.; Bartolini, A.; Garofalo, M.; Parrinello, M.; Tosatti, E. *Surf. Sci.* **1987**, *189/190*, 636.

(13) Sturmat, M.; Koch, R.; Rieder, K. H. *Phys. Rev. Lett.* **1996**, *77*, 5071.

(14) Robinson, I. K.; Eng, P. J.; Romainczyk, C.; Kern, K. *Phys. Rev. B* **1993**, *47*, 10700.

(15) Gritsch, T.; Coulman, D.; Behm, R. J.; Ertl, G. *Surf. Sci.* **1991**, *257*, 297.

(16) Buongiorno Nardelli, M.; Cvetko, D.; De Renzi, V.; Floreano, L.; Gotter, R.; Morgante, A.; Peloi, M.; Tommasini, F.; Danieli, R.; Rossini, S.; Taliani, C.; Zamboni, R. *Phys. Rev. B* **1996**, *53*, 1095; *Synth. Met.* **1996**, *76*, 173.

(17) Prato, S.; Floreano, L.; Cvetko, D.; De Renzi, V.; Morgante, A.; Modesti, S.; Biscarini, F.; Zamboni, R.; Taliani, C. *J. Phys. Chem. B* **1999**, *103*, 7788.

(18) Gross, L.; Seidel, C.; Fuchs, H. *Org. Electron.* **2002**, *3*, 7.

(19) Menozzi, C.; Corradini, V.; Cavallini, M.; Biscarini, F.; Betti, M. G.; Mariani, C. *Thin Solid Films* **2003**, *428*, 227.

(20) Evangelista, F.; Ruocco, A.; Corradini, V.; Donzello, M. P.; Mariani, C.; Betti, M. G. *Surf. Sci.* **2003**, *531*, 123.

(21) Garofalo, M.; Tosatti, E.; Ercolessi, F. *Surf. Sci.* **1987**, *188*, 321.

(22) Cvetko, D.; Lausi, A.; Morgante, A.; Tommasini, F.; Prince, K. C.; Sastry, M. *Meas. Sci. Technol.* **1992**, *3*, 997.

(23) A presentation of both the beamline and the branchline can be found at http://www.tasc.infm.it/tasc/lds/aloisa/aloisa.html.

(24) Floreano, L.; Naletto, G.; Cvetko, D.; Gotter, R.; Malvezzi, M.; Marassi, L.; Morgante, A.; Santaniello, A.; Verdini, A.; Tommasini, F.; Tondello, G. *Rev. Sci. Instrum.* **1999**, *70*, 3855.

(25) Gotter, R.; Ruocco, A.; Morgante, A.; Cvetko, D.; Floreano, L.; Tommasini, F.; Stefani, G. *Nucl. Instrum. Methods Phys. Res. A* **2001**, *467−468*, 1468.

(26) Ottaviano, L.; Lozzi, L.; Ramondo, F.; Picozzi, P.; Santucci, S. *J. Electron Spectrosc. Relat. Phenom.* **1999**, *105*, 145.

(27) Giovanelli, L.; Von Schenck, H.; Sinner-Hettenbach, M.; Papagergiou, N.; Göthelid, M.; Le Lay, G. *Surf. Sci.* **200**1, *486*, 55.

(28) Dufour, G.; Poncey, C.; Rochet, F.; Roulet, H.; Sacchi, M.; De Santis, M.; De Crescenzi, M. *Surf. Sci.* **1994**, *319*.

(29) Niwa, Y.; Kobayashi, H.; Tsuchiya, T. *J. Chem. Phys.* **1974**, *60*, 799.

(30) Peisert, H.; Knupfer, M.; Fink, J. *Surf. Sci.* **2002**, *515*, 491.

(31) Papageorgiou, N.; Ferro, Y.; Salomon, E.; Allouche, A.; Layet, J. M.; Giovanelli, L.; Le Lay, G. *Phys. Rev. B* **2003**, *68*, 235105.

(32) Ruocco, A.; Evangelista, F.; Attili, A.; Donzello, M. P.; Betti, M. G.; Giovanelli, L.; Gotter, R. *J. Electron Spectrosc. Relat. Phenom.*, **2004**, *137−140*, 165.

(33) Stohr, J. *NEXAFS Spectroscopy*; Springer-Verlag: Berlin, 1992.

(34) Carniato, S.; Luo, Y.; Ågren, H. *Phys. Rev. B* **2001**, *63*, 085105.

(35) Vlieg, E. *J. Appl. Crystallogr.* **2000**, *33*, 401. The software is freely distributed at http://www.esrf.fr/computing/scientific/.

(36) Bernasconi, M.; Tosatti, E. *Surf. Sci. Rep.* **1993**, *17*, 363.

(37) Cvetko, D.; Lausi, A.; Morgante, A.; Tommasini, F.; Prince, K. C. *Surf. Sci.* **1992**, *269/270*, 68.

(38) Vilfan, I.; Villain, J. *Surf. Sci.* **1988**, *199*, 165; *Europhys. Lett.* **1990**, *12*, 523.

(39) We cannot exclude that the lack of diffraction peaks in HAS pattern partly reflects also the Debye−Waller attenuation due to the rms displacements of the organic molecules.

(40) Betti, M. G.; Evangelista, F.; Mariani, C.; Ruocco, A., to be published.